

Synchronizing chaotic maps using an arbitrary scalar signal

Mitrajit Dutta

Department of Mathematics and Statistics, University of New Hampshire, Durham, New Hampshire 03824, USA
 (Received 22 March 2004; revised manuscript received 31 May 2005; published 24 August 2005)

A method we call the *slide-and-match* algorithm is presented whereby any transmitter-receiver pair of identical, chaotic maps may be synchronized using almost any scalar function of the driving transmitter state, transmitted to the receiver as the synchronizing signal. No prior investigation of either the map or the signal generating function is required. In order to illustrate the concepts, numerical simulations of applications are presented.

DOI: 10.1103/PhysRevE.72.026217

PACS number(s): 05.45.Xt, 05.45.Gg, 05.45.Pq

Over the last decade, there has been considerable interest in the synchronization of chaotic systems [1,2], particularly on account of its potential application to communication [3–12]. In this context, the setup involves two identical systems described by the same set of nonlinear evolution equations (but with different initial conditions) that lead to the same chaotic attractor. A scalar signal stream (often a state variable) is transmitted from one of the two systems (the *transmitter*) to the other (the *receiver*), in the hope that it can be used to synchronize the receiver to the transmitter. Several techniques have been invented to achieve the actual synchronization [1,2,7,13–23].

While these methods often work, whether two dynamical systems successfully synchronize or not depends on the choice of both the driving signal and the synchronization algorithm. For example, when using the x coordinate value to synchronize two Rossler systems, the method described in Ref. [2] fails while a different method involving nonidentical subsystems succeeds [19]. However, given embedding [24–26], it would appear reasonable that the infinite time series of *almost any* scalar function (of the state variables) would be sufficient to completely determine the state of the system, and therefore be sufficient for synchronization [27]. In this paper, we present a method that achieves just that [28].

First, we clearly state the problem at hand. We have a pair of identical, chaotic, dynamical systems which we call the transmitter and the receiver. Their time- i state vectors are represented by \vec{X}_i and \vec{Y}_i , respectively. Let M represent the map that evolves the dynamical system. We restrict ourselves here to mixing, chaotic maps [29] with just one Lyapunov exponent positive, and the rest negative. We also have a scalar function $f(\vec{X})$ whose form is known to both the sides. When applied to the transmitter state vector, it generates the *signal* s_i which is transmitted to the receiver. When applied to the receiver state vector, it generates the *pseudosignal* which is visible to the synchronizing mechanism. Our objective is to present a scheme that uses the signal to synchronize the state of the receiver to that of the transmitter.

Consider the fate of an ϵ ball (of the same dimension as the dynamical system) of initial conditions centered at some \vec{Y}_0 , on \mathcal{A} , the chaotic attractor of M . Since M has only one positive Lyapunov exponent, and the rest are negative, evolution stretches the ϵ ball along one direction only while

shrinking it along all the others. To preserve finiteness, we truncate the ends at every iterate. After a sufficient number of iterates the image of the ϵ ball (see Fig. 1) looks like an essentially one-dimensional curve L_i , lying in \mathcal{A} , with \vec{Y}_i , the corresponding image of \vec{Y}_0 , contained within it. Thus follows the concept of the *local unstable manifold* at \vec{Y}_i corresponding to a semi-infinite orbit “ $\cdots\vec{Y}_{i-2}\vec{Y}_{i-1}\vec{Y}_i$.” Let C_i be a curve of finite length lying in \mathcal{A} and containing \vec{Y}_i . We then define its *local preimage* C_i^{-1} as the shortest curve, also lying in \mathcal{A} , and containing \vec{Y}_{i-1} , whose forward image is C_i . If C_i satisfies the additional property $\lim_{n \rightarrow \infty} C_i^{-n} = \vec{Y}_{i-n}$ (C_i^{-n} is the n th local preimage of C_i), then we identify C_i with L_i , (a section of) the local unstable manifold at \vec{Y}_i at iterate i [30]. An interesting property of the dynamics near L_i is that points in the vicinity of L_i converge onto L_i under iteration, although they diverge away from one another along L_i . We shall exploit this feature.

Since the transmitter and the receiver are identical systems with states evolving on identical chaotic attractors, ergodicity guarantees that \vec{X}_i and \vec{Y}_i will come arbitrarily close arbitrarily often. But we simply require that \vec{X}_i come close to *any part* of L_i —a situation far less restrictive and, consequently, more frequent. Once that occurs, further iteration

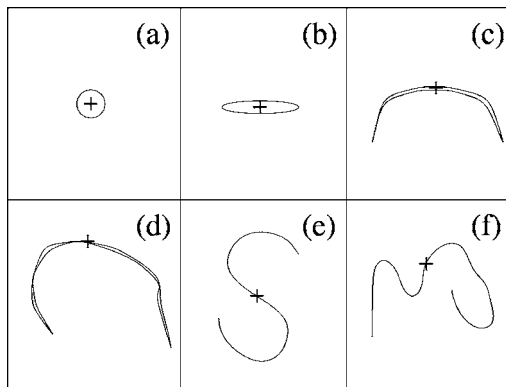


FIG. 1. The evolution of an ϵ ball for a dynamical system described by a discrete map with only one positive Lyapunov exponent and no zero Lyapunov exponents. The + symbol represents the state vector \vec{Y}_i .

will only bring L_i and \vec{X}_i progressively closer. Synchronization may then be achieved simply by sliding \vec{Y}_i along L_i to the part that is close to \vec{X}_i . The transmitted signal s_i is sufficient to identify this part. Thus follows the essence of our *slide-and-match* synchronization algorithm: *at each iterate, slide the receiver system along its local unstable manifold just far enough for the pseudosignal to match the transmitted signal.*

Note that since the receiver cannot see \vec{X}_i it cannot tell when L_i and \vec{X}_i are close enough for the prescription to be applied. However, since L_i lies in \mathcal{A} , sliding \vec{Y}_i along L_i by arbitrary distances, never pushes it off \mathcal{A} . Thus it is safe to leave the mechanism switched on at all times.

Symbolically, our slide-and-match synchronization scheme may be expressed as follows:

$$\text{Transmitter: } \vec{X}_i = M(\vec{X}_{i-1}); s_i = f(\vec{X}_i). \quad (1)$$

$$\text{Receiver: } \vec{Y}_{i-} = M(\vec{Y}_{i-1}); f(\vec{Y}_i) = s_i; \quad (2)$$

$$\vec{Y}_{i-} \in L_i; \vec{Y}_i \in L_i, \quad (3)$$

where \vec{Y}_{i-} and \vec{Y}_i represent the pre-slide and the post-slide receiver state vectors at iterate i . Solving $f(\vec{Y}_i) = s_i$ while simultaneously satisfying the condition $\vec{Y}_i \in L_i$ determines \vec{Y}_i . Equation (2) assumes that such a solution is available. Should no solution exist (this is typically the case during the initial transient before synchronization gets a chance to set in), then \vec{Y}_i is set equal to \vec{Y}_{i-} . In case of multiple solutions, we choose the one whose distance from \vec{Y}_{i-} , as measured along L_i , is the smallest [31].

Successful implementation of the proposed scheme is crucially contingent upon reliable and efficient computation of the local unstable manifold at each iterate. It would be easiest to approximate the manifold at each point as the local tangent vector, but such a linearized approach breaks down in the presence of very little noise. Including higher order Taylor expansion terms to better approximate the shape of L_i , or employing filtering techniques (using, perhaps, the Kalman filter [21,32]) might help, but are generally computationally expensive. Instead we adopt the following technique: we approximate the local unstable manifold at some \vec{Y}_i as a piecewise-straight line, \tilde{L}_i , with its middle vertex at \vec{Y}_i [33].

Given \tilde{L}_i , s_i , and \vec{Y}_{i-} , solving for \vec{Y}_i on \tilde{L}_i is straightforward. However, evolving \tilde{L}_i is complicated by the natural tendency of L_i (and therefore \tilde{L}_i) to both stretch and fold under iteration. Therefore, at each iterate i , we first pick a few points on \tilde{L}_{i-1} close to \vec{Y}_{i-1} ensuring that the piecewise-straight line defined by them satisfies the following conditions: (i) no segment is longer than a preset value, (ii) no two adjacent segments form an angle smaller than a preset value, and (iii) the total length of the line is sufficiently large compared to the *sliding distances*, i.e., the distances between the \vec{Y}_i 's and the \vec{Y}_{i-} 's as measured along the corresponding \tilde{L}_i 's.

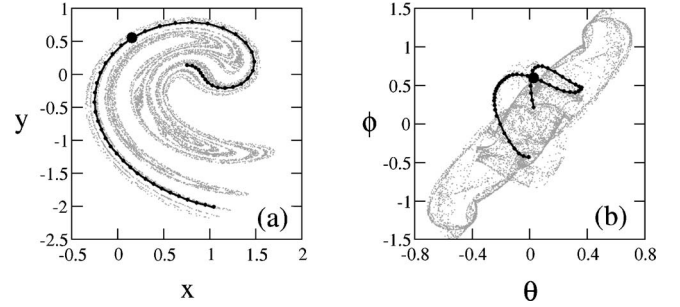


FIG. 2. Piecewise-linear approximations of the local, unstable manifold \tilde{L} using 50 segments. The large circles represent the state vector \vec{Y} , the small circles represent the other vertices, and the background shows the corresponding chaotic attractor. (a) The Ikeda map with $a=1$, $b=0.9$, $\kappa=0.4$, and $\eta=6.0$. (b) The forced, damped, double-pendulum system with $l=1$, $m=0.5$, $\mu_1=0.25$, $\mu_2=0.125$, $\rho=0.375$, and $\omega=\pi$. This is a five-dimensional system described by a four-dimensional map. The plot depicts a two-dimensional projection onto the θ - ϕ plane. θ and ϕ are plotted in radians.

The chosen points are then evolved using M to obtain \tilde{L}_i .

We now present two examples to illustrate our algorithm. First, we choose the Ikeda system. Denoting $\vec{X} \equiv (x, y)$ as its state vector, we can describe its evolution by the following two-dimensional map [34]:

$$x_{i+1} = a + b[x_i \cos(\theta_i) - y_i \sin(\theta_i)], \quad (4)$$

$$y_{i+1} = b[x_i \sin(\theta_i) + y_i \cos(\theta_i)], \quad (5)$$

where $\theta_i = \kappa - \eta / (1 + x_i^2 + y_i^2)$. We pick parameter values $a=1$, $b=0.9$, $\kappa=0.4$, and $\eta=6.0$. The corresponding chaotic attractor and a typical, piecewise linear approximation to the local unstable manifold are shown in Fig. 2(a). Figure 3 illustrates the synchronization of a pair of such systems using various scalar signals.

Our second example involves the forced, damped, double pendulum. This is a mechanical device consisting of a uniform rod suspended by a hinge from a second rod which is, in turn, suspended from a support by a second hinge (see Fig. 4). The rods (pendula) are free to swing in a vertical plane. θ and ϕ represent the deviations of the inner and the outer pendula from the vertical, while m_1, m_2 and l_1, l_2 represent their masses and lengths, respectively. Viscous dissipation is provided by linear friction at the hinges with μ_1 and μ_2 as the coefficients of friction (viscosity). An external forcing mechanism vertically oscillates the top support sinusoidally with amplitude ρ and frequency ω . Without loss of generality, we set $m_1 = l_1 = g = 1$ (g is the acceleration due to gravity), and drop the subscripts from m_2 and l_2 to obtain

$$\dot{\theta} = u, \quad (6)$$

$$\dot{\phi} = v, \quad (7)$$

$$\dot{u} = \frac{1}{D} \left[\left(\frac{l^2}{6} \right) F_1 - \left(\frac{ml \cos(\theta - \phi)}{4} \right) F_2 \right], \quad (8)$$

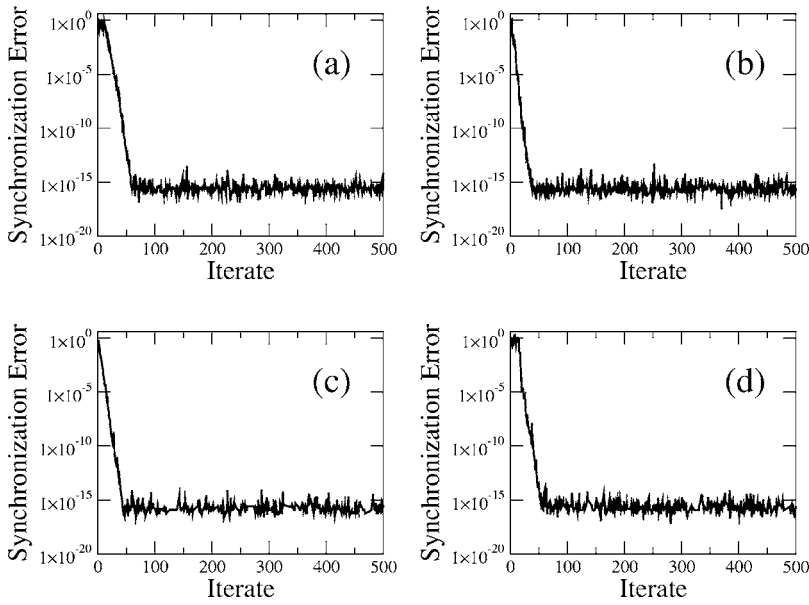


FIG. 3. The synchronization error, defined here as the Euclidean distance between the transmitter and receiver state vectors, is plotted as a function of the iterate number, thus illustrating the synchronization of two identical Ikeda systems for various signal-generating, scalar functions $f(\vec{X})$. At iterate 0, the transmitter and receiver state vectors are typically far apart. The parameter values are $a=1$, $b=0.9$, $\kappa=0.4$, and $\eta=6.0$. A little noise was added to prevent exact synchronization. (a) $f(\vec{X})=x$; (b) $f(\vec{X})=y$; (c) $f(\vec{X})=x^2+y^2$; (d) $f(\vec{X})=x^2-y^2$.

$$\dot{v} = \frac{1}{D} \left[\left(\frac{-l \cos(\theta - \phi)}{4} \right) F_1 + \left(\frac{3m + 1}{6} \right) F_2 \right], \quad (9)$$

where

$$F_1 = -mlv^2 \sin(\theta - \phi) - \tilde{g}(2m + 1) \sin(\theta) - 2\mu_1 u + 2\mu_2(v - u), \quad (10)$$

$$F_2 = lu^2 \sin(\theta - \phi) - \tilde{g}l \sin(\phi) - 2\mu_2(v - u)/m, \quad (11)$$

$$D = l^2(3m + 1)/9 - ml^2 \cos(\theta - \phi)^2/4, \quad (12)$$

$$\tilde{g} = 1 - \rho \omega^2 \sin(\omega t). \quad (13)$$

The time- $(2\pi/\omega)$ strobed Poincaré section reduces this five-dimensional system to a map with a four-dimensional state vector $\vec{X} \equiv (\theta, \phi, u, v)$, where all the quantities are measured at the beginning of every forcing cycle. We pick parameter values $l=1$, $m=0.5$, $\mu_1=0.25$, $\mu_2=0.125$, $\rho=0.375$, and $\omega = \pi$. The corresponding chaotic attractor and a typical, piece-

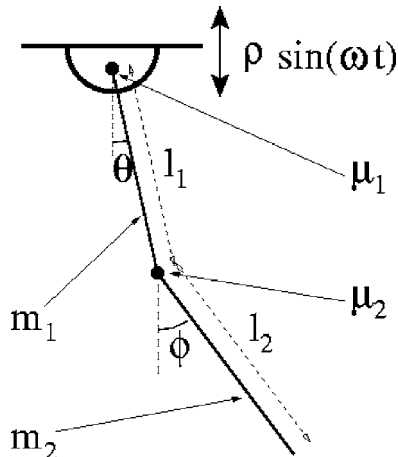


FIG. 4. The forced, damped, double pendulum.

wise linear approximation to the local unstable manifold are shown in Fig. 2(b), while the synchronization of a pair of such systems using various scalar signals is illustrated in Fig. 5.

The primary advantage of the slide-and-match synchronization scheme presented here is that it works for *any* pair of identical chaotic maps with one positive Lyapunov exponent (and the other Lyapunov exponents negative) and for *almost any* [35] scalar signal, the functional form of which is known to both sides. No detailed, prior investigation of either the map or the signal generating function is required. Furthermore, the complexity of the algorithm is independent of the system dimension. No matter how high the system dimension may be, the slide-and-match algorithm reduces synchronization to an essentially one-dimensional problem [36].

The proposed scheme shares a few similarities with some known methods for observer design [22,23] and synchronization [20]—they all exploit the intrinsic contraction and expansion properties of the underlying dynamics. However, an important difference is that our method provides for synchronization adjustments along the manifold, \tilde{L}_i , which is nonlinear and yet, easily implemented on the computer. Thus in order for our synchronization algorithm to succeed, it is sufficient for the transmitter state vector \vec{X}_i to come close to *any part* of \tilde{L}_i , rather than to the receiver state vector, \vec{Y}_i , specifically. Since \tilde{L}_i is a curve of positive length, this leads to quicker synchronization. By the same token, for synchronization to be destroyed, any noise in the system must be strong enough to push the entire \tilde{L}_i (not just \vec{Y}_i) away from \vec{X}_i . This improves the noise resistance, leading to fewer noise-induced desynchronization bursts.

Finally, the algorithm has the important, useful feature that in the course of the synchronization adjustments, the receiver state vector always remains on the chaotic attractor. This prevents it from escaping the basin of attraction of the chaotic attractor of interest before achieving synchronization.

The above advantages should make slide-and-match useful for practical applications requiring synchronization of

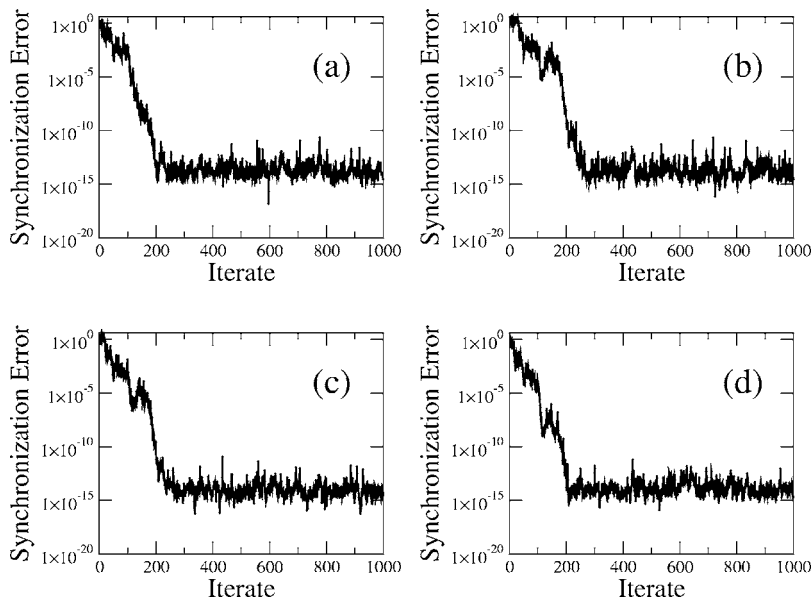


FIG. 5. The synchronization error, defined here as the Euclidean distance between the transmitter and receiver state vectors, is plotted as a function of the iterate number, thus illustrating the synchronization of two identical forced, damped, double pendula for various signal-generating, scalar functions $f(\vec{X})$. At iterate 0, the transmitter and receiver state vectors are typically far apart. The parameter values are $l=1$, $m=0.5$, $\mu_1=0.25$, $\mu_2=0.125$, $\rho=0.375$, and $\omega=\pi$. A little noise was added to prevent exact synchronization. (a) $f(\vec{X})=\sin(\theta)$; (b) $f(\vec{X})=\sin(\phi)$; (c) $f(\vec{X})=u \cos(\theta)$; (d) $f(\vec{X})=v \cos(\phi)$.

chaos, e.g., communication with chaos, observer design. However, a disadvantage of the method is that it almost certainly requires a computer as part of the setup, while many of the other methods present in literature may be implemented using much simpler components.

Summing up, we have presented a different synchronization scheme that synchronizes two chaotic maps using almost any scalar signal. We expect the fundamental principle underlying the method to hold good for hyperchaotic systems with multiple positive Lyapunov exponents, as well. That is, we expect that adjustments along just the local unstable manifold should be sufficient for synchronization.

Thus the complexity of the algorithm is expected to be determined by the dimensionality of the local unstable manifold only rather than by that of the complete dynamical system—a significant simplification for high-dimensional systems. Unfortunately, the previously mentioned difficulties associated with the stretching and the folding of the local unstable manifold prove severe when the local unstable manifold needs to be approximated by a multidimensional mesh rather than by a piecewise-straight line. This makes the software implementation of generalized *slide-and-match* synchronization for hyperchaotic systems challenging, and will be the subject of future work.

-
- [1] H. Fujisaka and T. Yamada, *Prog. Theor. Phys.* **69**, 32 (1983).
 [2] L. M. Pecora and T. L. Carroll, *Phys. Rev. Lett.* **64**, 821 (1990); *Phys. Rev. A* **44**, 2374 (1991).
 [3] S. Hayes, C. Grebogi, and E. Ott, *Phys. Rev. Lett.* **70**, 3031 (1993).
 [4] S. Hayes, C. Grebogi, E. Ott, and A. Mark, *Phys. Rev. Lett.* **73**, 1781 (1994).
 [5] K. M. Cuomo and A. V. Oppenheim, *Phys. Rev. Lett.* **71**, 65 (1993).
 [6] L. Kocarev, K. S. Halle, K. Eckert, L. O. Chua, and U. Parlitz, *Int. J. Bifurcation Chaos Appl. Sci. Eng.* **2**, 709 (1992).
 [7] L. Kocarev and U. Parlitz, *Phys. Rev. Lett.* **74**, 5028 (1995).
 [8] Y.-C. Lai, E. Bollt, and C. Grebogi, *Phys. Lett. A* **255**, 75 (1999).
 [9] M. Hasler, *Int. J. Bifurcation Chaos Appl. Sci. Eng.* **8**, 647 (1998).
 [10] T. L. Carroll, *Phys. Rev. E* **67**, 026207 (2003).
 [11] A. Uchida, M. Kawano, and S. Yoshimori, *Phys. Rev. E* **68**, 056207 (2003).
 [12] R. Mislovaty, E. Klein, I. Kanter, and W. Kinzel, *Phys. Rev. Lett.* **91**, 118701 (2003).
 [13] C. W. Wu and L. O. Chua, *Int. J. Bifurcation Chaos Appl. Sci. Eng.* **3**, 1619 (1993).
 [14] U. Parlitz, L. Kocarev, T. Stojanovski, and H. Preckel, *Phys. Rev. E* **53**, 4351 (1996).
 [15] L. Kocarev, U. Parlitz, and T. Stojanovski, *Phys. Lett. A* **217**, 280 (1996).
 [16] S. Fahy and D. R. Hamann, *Phys. Rev. Lett.* **69**, 761 (1992).
 [17] R. E. Amritkar and N. Gupte, *Phys. Rev. E* **47**, 3889 (1993).
 [18] T. Stojanovski, L. Kocarev, and U. Parlitz, *Phys. Rev. E* **54**, 2128 (1996).
 [19] M. Ding and E. Ott, *Phys. Rev. E* **49**, R945 (1994).
 [20] L. Junge and U. Parlitz, *Phys. Rev. E* **64**, 055204 (2001).
 [21] E. E. N. Macau, C. Grebogi, and Y.-C. Lai, *Phys. Rev. E* **65**, 027202 (2002).
 [22] P. So, E. Ott, and W. P. Dayawansa, *Phys. Lett. A* **176**, 421 (1993).
 [23] P. So, E. Ott, and W. P. Dayawansa, *Phys. Rev. E* **49**, 2650 (1994).
 [24] F. Takens, *Detecting Strange Attractors in Turbulence*, Lecture Notes in Math No. 898 (Springer-Verlag, Berlin, 1981).
 [25] N. H. Packard, J. P. Crutchfield, J. D. Farmer, and R. S. Shaw, *Phys. Rev. Lett.* **45**, 712 (1980).
 [26] T. Sauer and J. A. Yorke, *Int. J. Bifurcation Chaos Appl. Sci. Eng.* **3**, 737 (1993).
 [27] T. Stojanovski, U. Parlitz, L. Kocarev, and R. Harris, *Phys.*

- Lett. A **233**, 355 (1997).
- [28] M. Dutta, Ph.D. thesis, University of Maryland, College Park, 2000.
- [29] We assume that our chaotic system is “mixing” in the limited sense that for any point A in the attractor, the trajectories corresponding to any two typical initial conditions occasionally come very close to A simultaneously.
- [30] For invertible M , the local unstable manifold at any point \vec{Y} on the chaotic attractor is uniquely defined independent of any orbit, since invertibility guarantees a unique orbit that leads to the point \vec{Y} at any given iterate.
- [31] The only points where one has difficulty computing \vec{Y}_i are the points where the local unstable manifold and the $f=\text{const}$ surfaces are tangent.
- [32] R. E. Kalman, J. Basic Eng. **83**, 35 (1960).
- [33] The slide-and-match algorithm for synchronization is not restricted to using the piecewise-linear approximation to the local unstable manifold. The problem of determining a suitable approximation to L_i is completely independent of the synchronization algorithm where we simply use L_i .
- [34] E. Ott, *Chaos in Dynamical Systems* (Cambridge University Press, Cambridge, England, 1993), p. 278.
- [35] We need only one technical assumption that almost every scalar function satisfies: it cannot be constant on any segment of the unstable manifold. A note for symmetric systems: if a system is invariant under a certain transformation, and the signal shares this invariance, then the receiver state may “synchronize” to either the true transmitter state or one of its symmetric counterparts. For example, for the forced, damped, double pendulum which is invariant under $(\theta, \phi, u, v) \rightarrow (-\theta, -\phi, -u, -v)$, using $\cos(\theta)$ as the signal could lead to the mentioned situation.
- [36] There is a caveat associated with this point. Clearly, the success of the synchronization algorithm presented in this paper is contingent upon the one-dimensional nature of the local unstable manifold. On average, this condition is indeed satisfied by chaotic maps with just one Lyapunov exponent positive,

and the others all negative. However, even for such systems, the local, unstable manifold may, at places, be multidimensional. For example, it is possible for the chaotic attractor \mathcal{A} to have embedded within it unstable periodic orbits with multidimensional, unstable manifolds. Therefore when the transmitter state vector \vec{X}_i and consequently the receiver state vector \vec{Y}_i come close to such an embedded periodic orbit, multiple degrees of freedom are generally necessary in order to appropriately slide \vec{Y}_i close to \vec{X}_i and maintain synchronization. Under such circumstances, the piecewise linear approximation to the local unstable manifold proves inadequate. Consequently, the distance between \vec{X}_i and \vec{Y}_i then increases. Fortunately, for systems with a single positive Lyapunov exponent (with the remaining Lyapunov exponents all negative), the time spent in such regions of multidimensional, local unstable manifolds is typically small. Therefore before the distance between \vec{X}_i and \vec{Y}_i grows too large, the systems typically return to regions with single-dimensional, local unstable manifolds. Then, the synchronization algorithm presented in this paper quickly brings \vec{Y}_i close to \vec{X}_i once again. This entire process manifests itself as a spike in the synchronization error, $\|\vec{X}_i - \vec{Y}_i\|$. Many such spikes are visible in Figs. 3 and 5. If the experiment is run for a very long time, then it is likely that a situation will be encountered where the systems spend a relatively long time in a region with a multidimensional, unstable manifold (e.g., imagine if \vec{X}_i and \vec{Y}_i happen to come very close to one of the aforementioned unstable periodic orbits embedded within \mathcal{A}). Then the distance between \vec{X}_i and \vec{Y}_i can grow large and break synchronization. But the time interval between such desynchronization bursts will be long provided the noise inherent in the setup (this is what determines the typical synchronization error) remains small. For a proper remedy to this problem one must use a multidimensional approximation to the local unstable manifold rather than the piecewise linear approximation described in this paper. A more detailed reference to this is included in the last paragraph.